Journal of Solid State Chemistry **159,** 198–203 (2001)
doi:10.1006/jssc.2001.9151, available online at http://www.idealibrary.com on IDEAL®

Organically Templated Zirconium Fluorides: Hydrothermal Syntheses, Structural Relationships, and Thermal Behavior of $(C_2H_{10}N_2)Zr_2F_{10}\cdot H_2O$ and $(C_4H_{12}N_2)ZrF_6\cdot H_2O$

Richard E. Sykora,* Michael Ruf,† and Thomas E. Albrecht-Schmitt*, [1]

**Department of Chemistry, Auburn University, Auburn, Alabama 36849; and †Bruker AXS, 5465 East Cheryl Parkway, Madison, Wisconsin 53711*

Received December 21, 2000; in revised form March 7, 2001; accepted March 15, 2001; published online May 11, 2001

The organically templated Zr(IV) fluorides, $(C_2H_{10}N_2)Zr_2F_{10}\cdot H_2O$ (AU2-6) and $(C_4H_{12}N_2)ZrF_6\cdot H_2O$ (AU1-6) have been prepared from the reaction of ZrO_2 with HF and ethylenediamine or piperazine under mild hydrothermal conditions. These compounds were characterized by single-crystal X-ray diffraction, DSC, TGA, and elemental analysis. AU2-6 consists of dodecahedral ZrF_8 units that share three edges with neighboring dodecahedra to form $^2_\infty[Zr_2F_{10}]^{2-}$ sheets that are separated by diprotonated ethylenediamine cations. AU1-6 contains edge-sharing ZrF_8 dodecahedra that form $^1_\infty[ZrF_6]^{2-}$ chains that further hydrogen bond with diprotonated piperazinium cations and water molecules. Application of dimensional reduction theory demonstrates that $^1_\infty[ZrF_6]^{2-}$ chains can be derived from the $^2_\infty[Zr_2F_{10}]^{2-}$ parent structure through the addition of one equivalent of fluoride. Thermal analyses indicate that the water molecules in AU2-6 are more tightly bound than those in AU1-6 as endotherms corresponding to water loss occur at 226 and 117°C in AU2-6 and AU1-6, respectively. Crystallographic data: AU2-6, monoclinic, space group $P2_1/n$, $a = 6.164(1)$, $b = 15.612(3)$, $c = 11.227(2)$ Å, $\beta = 95.31(3)^\circ$, $Z = 4$, Mo$K\alpha$, $\lambda\cdot 0.71073$, $R(F) = 2.94\%$ for 155 parameters with 3294 reflections with $I > 2\sigma(I)$; AU1-6, monoclinic, space group $C2/m$, $a = 12.190(5)$, $b = 12.732(6)$, $c = 6.356(2)$ Å, $\beta = 107.64(3)^\circ$, $Z = 4$, Mo$K\alpha$, $\lambda = 0.71073$, $R(F) = 1.68\%$ for 77 parameters with 869 reflections with $I > 2\sigma(I)$. © 2001 Academic Press

INTRODUCTION

High-valent early transition metals, lanthanides, and actinides display considerable variation in coordination number, geometry, and in some cases, oxidation state, making them logical choices for building structural flexibility in hydrothermal syntheses (1–12). Zirconium fluorides illustrate this principle well with molecular, one-, two-, and three-dimensional compounds being known where the coordination number of the Zr(IV) varies from six to eight (13). Aside from fundamental interests, zirconium fluorides are currently under investigation for applications ranging from flame retardants to NLO materials (14, 15). However, the preparative chemistry of these compounds is fraught with a number of synthetic challenges, the most important of which is that most solution-based routes lead to product mixtures (16, 17), impeding both the understanding of basic chemical processes and physical property measurements.

Our recent studies on the hydrothermal syntheses of organically templated low-dimensional U(IV) fluorides (6, 8) and aquofluorides (9) has prompted us to explore similar chemistry with Zr(IV) as has been accomplished in high-temperature solid-state reactions between UF_4 or ZrF_4 and alkali metal fluorides (18). Abrahams and coworkers have recently reported improved methods for isolating single-phase materials for several zirconium fluorides with known inorganic structural features (17). However, systematic investigation of materials synthesis via the combination of compositional diagrams with mild hydrothermal reaction conditions offers several advantages over conventional synthetic methods, especially in regard to determination of factors leading to the formation of multiple products from a fixed set of reactants (5, 9, 19–22). Furthermore, this methodology often provides access to high yields of pure phases, and most importantly, to superb conditions for the growth of large single crystals (23, 24). The latter will play a key role in the development of these compounds as NLO materials.

Herein we report the hydrothermal syntheses, structural relationships, and thermal behavior of the Zr(IV) fluorides $(C_2H_{10}N_2)Zr_2F_{10}\cdot H_2O$ (**AU2-6**) and $(C_4H_{12}N_2)ZrF_6\cdot H_2O$ (**AU1-6**). These compounds bridge the gap between hydrothermal actinide chemistry and the chemistry of early transition metals. **AU2-6** also provides the first example of a layered zirconium fluoride with an organic structure-directing amine.

---

[1] To whom correspondence should be addressed. E-mail: albreth@auburn.edu. Tables of anisotropic displacement parameters, hydrogen atom coordinates, and structure factors for **AU2-6** and **AU1-6** (35 pages) are available from the corresponding author upon request.

0022-4596/01 $35.00
Copyright © 2001 by Academic Press
All rights of reproduction in any form reserved.

EXPERIMENTAL

Syntheses

ZrO_2 (99%, Alfa-Aesar), HF (48 wt%, Aldrich), piperazine (99%, Aldrich), and ethylenediamine (99.5%, Aldrich) were used as received. Distilled and millipore filtered water was used in all reactions. The resistance of the water was 18.2 MOhm. Elemental (CHN) microanalyses were performed by Atlantic Microlab, Inc. Reactions were run in Parr 4749 23-ml autoclaves with PTFE liners. The naming system for these compounds stands for Auburn University, the dimensionality of the structure, and the compound number (6, 8, 9).

*$(C_2H_{10}N_2)Zr_2F_{10}\cdot H_2O$ (**AU2-6**).* ZrO_2 (370 mg, 3 mmol) and ethylenediamine (0.07 mL, 1 mmol) were loaded in a 23-ml PTFE-lined autoclave. Water (2 ml) was then added to the mixture followed by the drop-wise addition of HF (0.58 ml, 16 mmol). The autoclave was sealed and placed in a box furnace that had been preheated to 180°C. After 72 h the furnace was cooled at 9°C/h to 23°C. The product consisted of a clear and colorless liquid over a large rosette of approximately hexagonal, colorless tablets. The mother liquor was decanted from the crystals, which were then washed with methanol and allowed to dry; yield, 540 mg, 78% (based on Zr). [Analysis, Calculated for $C_2H_{12}N_2F_{10}OZr_2$: C, 5.31; H, 2.67; N, 6.19. Found: C, 5.35; H, 2.61; N, 6.02.]

*$(C_4H_{12}N_2)ZrF_6\cdot H_2O$ (**AU1-6**).* ZrO_2 (246 mg, 2 mmol) and piperazine (345 mg, 4 mmol) were loaded in a 23-ml PTFE-lined autoclave. Water (1-ml) was then added to the solids followed by the drop-wise addition of HF (0.51 ml, 14 mmol). The autoclave was sealed and placed in a box furnace that had been preheated to 180°C. After 72 h the furnace was cooled at 9°C/h to 23°C. The product consisted of a clear and colorless liquid over very large colorless prisms, one of which measured 3.5 × 1.5 × 13 mm. The mother liquor was decanted from the crystals, which were then washed with methanol and allowed to dry; yield, 520 mg, 84% (based on Zr). [Analysis. Calculated for $C_4H_{14}N_2F_6OZr$: C, 15.43; H, 4.53; N, 9.00. Found: C, 15.46; H, 4.35; N, 9.07.]

Crystallographic Studies

Intensity data were collected from single crystals of **AU1-6** with the use of a Nicolet R3M diffractometer. The data for **AU2-6** were collected with a Bruker SMART APEX CCD system. Crystals of **AU2-6** and **AU1-6** are nonproblematic and diffract remarkably well. Data for all compounds were processed and analytical absorption corrections were applied. The structures were solved by direct methods and refined using the SHELXTL-93 package (25). In these refinements, hydrogen atom positions were calculated with isotropic riding temperature factors. While many of the hydrogen positions in **AU1-6** could be located from difference maps, calculated positions were used for uniformity in the piperazinium dication. The hydrogen position(s) for the water molecule in **AU1-6** were located from the difference map. Some crystallographic details are listed in Table 1 for **AU2-6** and **AU1-6**. The final positional parameters for **AU2-6** and **AU1-6** are given in Tables 2 and 3. Additional

TABLE 1
Crystallographic Data for $(C_2H_{10}N_2)Zr_2F_{10}\cdot H_2O$ (AU2-6) and $(C_4H_{12}N_2)ZrF_6\cdot H_2O$ (AU1-6)

Formula	$(C_2H_{10}N_2)Zr_2F_{10}\cdot H_2O$	$(C_4H_{12}N_2)ZrF_6\cdot H_2O$
Formula mass (amu)	452.57	311.39
Color and habit	Colorless, prism	Colorless, hexagonal tablet
Space group	$P2_1/n$ (No. 14)	$C2/m$ (No. 12)
a(Å)	6.164(1)	12.190(5)
b(Å)	15.612(3)	12.732(6)
c(Å)	11.227(2)	6.356(2)
β(deg.)	95.31(3)	107.64(3)
V(Å^3)	1075.7(4)	940.1(7)
Z	4	4
T(°C)	22	22
λ(Å)	0.710 73	0.710 73
Maximum 2θ (deg.)	68.90	50.10
Observed data $I > 2\sigma(I)$	3294	869
ρ_{calcd} (g cm^{-3})	2.782	2.200
μ(Mo$K\alpha$) (cm^{-1})	20.66	12.36
$R(F)$ for $F_o^2 > 2\sigma(F_o^2)^a$	0.0294	0.0168
$R_w(F_o^2)^b$	0.0688	0.0454

$^a R(F) = \sum||F_o| - |F_c||/\sum|F_o|$.
$^b R_w(F_o^2) = [\sum[w(F_o^2 - F_c^2)^2]/\sum wF_o^4]^{1/2}$.

TABLE 2
Atomic Coordinates and Equivalent Isotropic Displacement Parameters for $(C_2H_{10}N_2)Zr_2F_{10}\cdot H_2O$ (AU2-6)

Atom	x	y	z	U_{eq} (Å^2)^a
Zr(1)	− 0.0644(1)	0.7426(1)	0.2526(1)	0.011(1)
Zr(2)	− 0.5324(1)	0.7464(1)	0.4301(1)	0.011(1)
F(1)	0.1410(2)	0.7488(1)	0.1164(1)	0.019(1)
F(2)	0.2020(2)	0.6697(1)	0.3436(1)	0.018(1)
F(3)	− 0.1485(2)	0.6231(1)	0.2224(1)	0.024(1)
F(4)	0.2028(2)	0.8184(1)	0.3371(1)	0.018(1)
F(5)	− 0.1583(2)	0.8659(1)	0.2308(1)	0.022(1)
F(6)	− 0.1618(2)	0.7416(1)	0.4254(1)	0.018(1)
F(7)	− 0.4348(2)	0.7421(1)	0.2580(1)	0.018(1)
F(8)	− 0.4427(2)	0.8681(1)	0.4490(1)	0.024(1)
F(9)	− 0.4500(2)	0.6233(1)	0.4638(1)	0.022(1)
F(10)	− 0.7428(2)	0.7522(1)	0.5647(1)	0.019(1)
N(1)	− 0.0472(4)	0.5914(1)	− 0.3947(2)	0.029(1)
N(2)	− 0.0623(4)	− 0.0980(1)	0.5873(2)	0.029(1)
C(1)	0.0721(4)	0.5211(2)	− 0.4498(2)	0.024(1)
C(2)	0.0707(4)	− 0.0371(2)	0.5230(2)	0.029(1)
O(1)	0.3941(3)	0.4997(1)	0.2986(2)	0.032(1)

^{a} U_{eq} is defined as one-third of the trace of the orthogonalized $\mathbf{U}_{ij}$ tensor.

TABLE 3
Atomic Coordinates and Equivalent Isotropic Displacement Parameters for $(C_4H_{12}N_2)ZrF_6 \cdot H_2O$ (AU1-6)

Atom	x	y	z	U_{eq} (Å^2)[a]
Zr(1)	0.0917(1)	0	− 0.2035(1)	0.015(1)
F(1)	0	0.0933(1)	$-\frac{1}{2}$	0.023(1)
F(2)	0.2051(1)	0	− 0.3779(2)	0.025(1)
F(3)	0.0717(1)	0	0.1754(2)	0.022(1)
F(4)	0.1126(1)	0.1509(1)	− 0.1087(2)	0.030(1)
F(5)	0.2509(1)	0	0.0453(3)	0.037(1)
N(1)	0.2142(2)	0.1701(1)	0.3388(3)	0.033(1)
C(1)	0.1493(2)	0.2701(2)	0.3158(3)	0.036(1)
C(2)	0.3380(2)	0.1837(2)	0.4615(4)	0.036(1)
O(1)	0.4694(4)	0	0.2016(8)	0.106(2)

[a] U_{eq} is defined as one-third of the trace of the orthogonalized U_{ij} tensor.

crystallographic details are available as auxiliary material. (see footnote 1).

Thermal Analysis

Thermal data for **AU2-6** and **AU1-6** were collected using a TA Instruments, Model 2920 Differential Scanning Calorimeter (DSC) and a Perkin–Elmer Pyris 1 Thermogravimetric Analyzer (TGA). Samples (10–20 mg) were encapsulated in aluminum pans and heated at 10°C/min from 25 to 600°C under a nitrogen atmosphere.

RESULTS AND DISCUSSION

Syntheses

The hydrolysis of ZrO_2 through reaction with HF in the presence of the structure-directing amines, ethylenediamine, or piperazine under mild hydrothermal conditions results in the formation of $(C_2H_{10}N_2)Zr_2F_{10} \cdot H_2O$ (**AU2-6**) and $(C_4H_{12}N_2)ZrF_6 \cdot H_2O$ (**AU1-6**). These compounds are the result of investigations of compositional diagrams bordered by 50% ZrO_2, 50% amine, and 100% HF. In both cases only single products were isolated in these regions. The vastly reduced complexity of the compositional diagrams for the zirconium systems versus those of uranium is explained by both the redox character of uranium, which allows for U(IV) and U(VI), and uranium's increased size, making UF_9 units common. Coordination numbers beyond eight are rare for zirconium fluorides (excluding cluster compounds with interstitial fluoride) (18). Redox processes are essentially absent from zirconium fluorides, which actually abridges the chemistry in a fortuitous manner and provides a high yield route to pure phases in the form of large single crystals. The product composition was not significantly affected by changes in the amount of water employed or by increasing the reaction temperature to 200°C. However, larger crystals of **AU2-6** (up to 0.5 × 7 × 7 mm) were isolated when the water content was increased from 1 ml to 3 ml.

Structures

$(C_2H_{10}N_2)Zr_2F_{10} \cdot H_2O$ (AU2-6). **AU2-6** is a layered compound containing $^{2}_{\infty}[Zr_2F_{10}]^{2-}$ slabs separated by diprotonated ethylenediamine and water molecules. Each layer consists of two independent ZrF_8 dodecahedra that share three edges with neighboring polyhedra. These polyhedra are depicted in Fig. 1a. This is a new structural motif for layered zirconium fluorides not observed before with other organic or inorganic cations. Previously reported two-dimensional zirconium fluorides typically contain polyhedra that share both corners and edges (26–29). The uniqueness

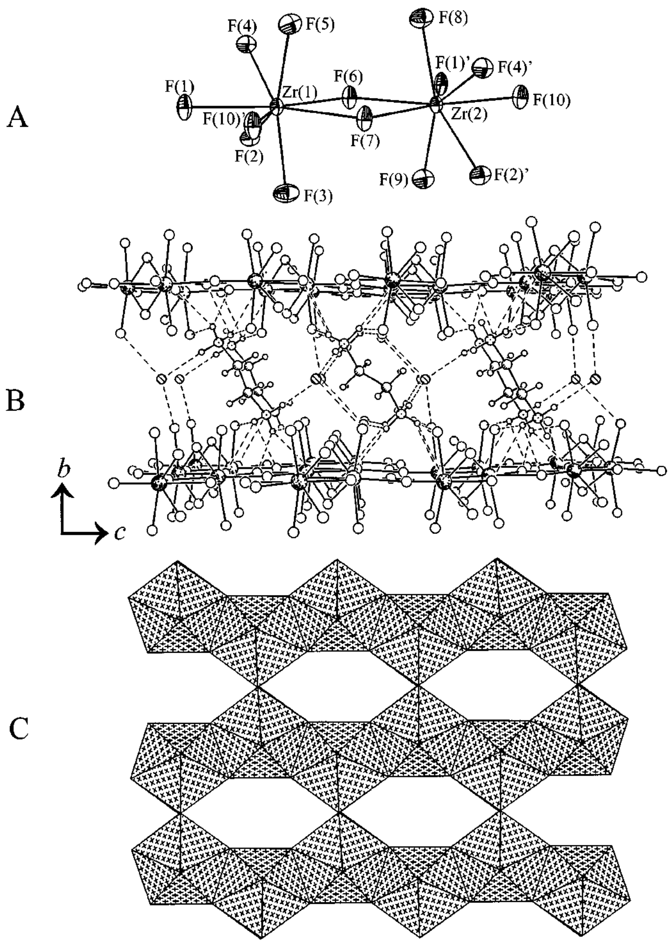

FIG. 1. **AU2-6** (a) Edge-sharing of $[ZrF_8]$ dodecahedra with atom labeling scheme. Fifty-percent probability ellipsoids are shown. (b) A view along the *a* axis showing the layered structure with hydrogen bonding network containing ethylenediamine dications and water molecules that separate the layers. (c) A polyhedral representation of a $^{2}_{\infty}[Zr_2F_{10}]^{2-}$ layer showing edge-sharing ZrF_8 dodecahedra.

TABLE 4
Selected Bond Distances (Å) for $(C_2H_{10}N_2)Zr_2F_{10}\cdot H_2O$ (AU2-6)

Zr(1)–F(1)	2.076(1)	Zr(2)–F(1)′	2.260(2)
Zr(1)–F(2)	2.173(1)	Zr(2)–F(2)′	2.182(1)
Zr(1)–F(3)	1.958(1)	Zr(2)–F(4)′	2.168(1)
Zr(1)–F(4)	2.174(1)	Zr(2)–F(6)	2.291(1)
Zr(1)–F(5)	2.018(1)	Zr(2)–F(7)	2.077(1)
Zr(1)–F(6)	2.083(1)	Zr(2)–F(8)	1.985(1)
Zr(1)–F(7)	2.290(1)	Zr(2)–F(9)	2.015(1)
Zr(1)–F(10)′	2.288(2)	Zr(2)–F(10)	2.082(1)
	Hydrogen bonding distances		
N(1)···F(5)	2.748(5)	O(1)···N(1)	2.862(5)
N(1)···F(9)	2.864(5)	O(1)···N(2)	2.859(5)
N(2)···F(3)	2.871(5)	O(1)···F(5)	2.689(5)
N(2)···F(8)	2.741(5)	O(1)···F(9)	2.785(5)

of this inorganic architecture is indicative of the structure-directing nature of the ethylenediamine dications.

In **AU2-6**, there are two crystallographically unique Zr sites. Polyhedra containing Zr(1) are surrounded solely by Zr(2) and vice versa. Each polyhedra contains two terminal fluorides, F(3) and F(5) for Zr(1), and F(8) and F(9) for Zr(2). These nonbridging ligands point between layers and participate in strong hydrogen bonding with the diprotonated ethylenediamine. A view along the *a* axis, showing the layered structure with the diprotonated ethylenediamine separating the layers, is depicted in Fig. 1b. A polyhedral representation of a ${}^{2}_{\infty}[Zr_2F_{10}]^{2-}$ layer showing edge-sharing ZrF_8 dodecahedra is depicted in Fig. 1c. Zr–F bond distances range from 1.958(1) to 2.018(1) Å for terminal fluorides, and from 2.076(1) to 2.291(1) Å for bridging fluorides. The O(1) atom from the water molecule forms four hydrogen bonds in an approximately tetrahedral arrangement. Selected bond distances are given in Table 4.

$(C_4H_{12}N_2)ZrF_6\cdot H_2O$ (AU1-6). **AU1-6** is composed of ${}^{1}_{\infty}[ZrF_6]^{2-}$ chains constructed from dodecahedral $[ZrF_8]$ units (Fig. 2a) that share opposite edges with neighboring polyhedra. These chains extend along the *c* axis and are separated by piperazinium dications and water molecules, all of which form a hydrogen bonding network as depicted in Fig. 2b. A polyhedral representation of this chain is depicted in Fig. 2c. As each polyhedron has two such edge-sharing arrangements, the coordination environment around each Zr(IV) center can be described as $[ZrF_{4/2}F_4]^{2-}$. The Zr–F bridging and terminal distances range from 2.053(2) to 2.493(2) Å and 2.007(1) to 2.099(2) Å, respectively. Selected bond distances are given in Table 5.

Structural Relationships

Rationalizing and predicting changes in the architecture of crystalline solids can be accomplished in many cases through the application of the dimensional reduction formalism (30–34), which was originally termed depolymerization by Penneman *et al.* in reference to the reactions of alkali metal fluorides with thorium and uranium fluorides (18). Long and Tulsky have compiled a searchable database demonstrating that the structures of numerous

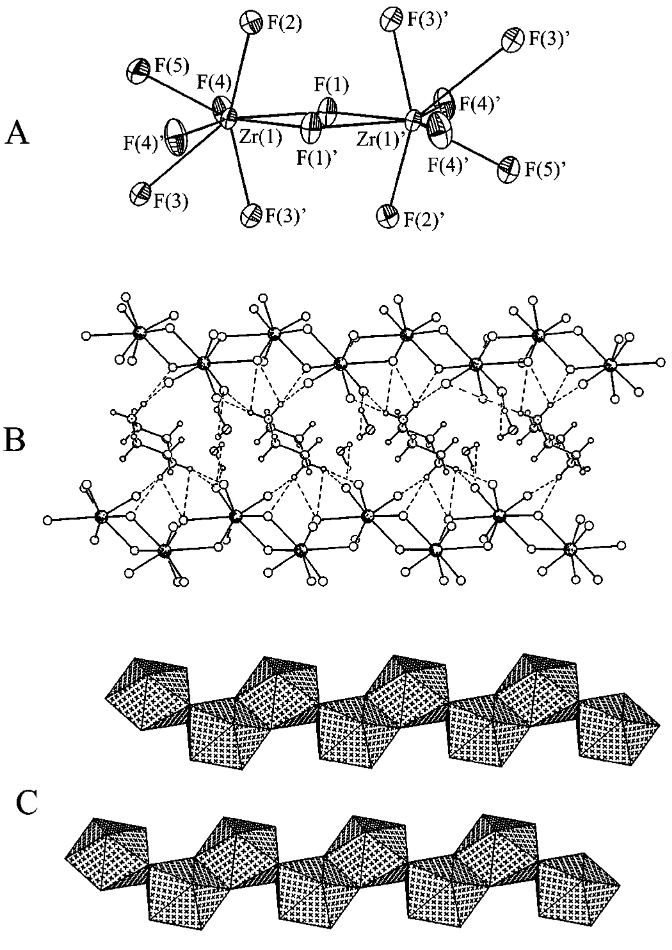

FIG. 2. **AU1-6** (a) Edge-sharing $[ZrF_8]$ dodecahedra with atom labeling scheme. Fifty-percent probability ellipsoids are shown. (b) ${}^{1}_{\infty}[ZrF_{4/2}F_4]^{2-}$ chains separated by piperazine dications, water molecules, and the resulting hydrogen bonding network. (c) A polyhedral representation of a ${}^{1}_{\infty}[ZrF_{4/2}F_4]^{2-}$ chain.

TABLE 5
Selected Bond Distances (Å) for $(C_4H_{12}N_2)ZrF_6\cdot H_2O$ (AU1-6)

Zr(1)–F(1) (×2)	2.221(1)	Zr(1)–F(3)′	2.053(2)
Zr(1)–F(2)	2.017(2)	Zr(1)–F(4) (×2)	2.007(1)
Zr(1)–F(3)	2.493(2)	Zr(1)–F(5)	2.099(2)
	Hydrogen bonding distances		
N(1)···F(2)	2.840(3)	N(1)···F(5)	2.979(3)
N(1)···F(3)	2.773(3)	O(1)···F(5)	2.545(3)
N(1)···F(4)	2.747(3)		

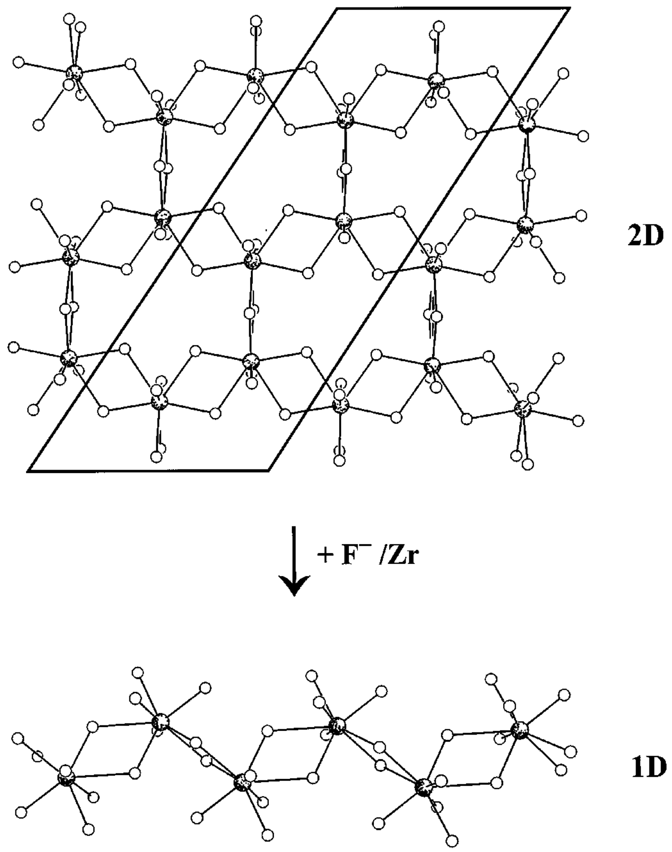

FIG. 3. Dimensional reduction of a ${}^{2}_{\infty}[\mathrm{Zr_2F_{10}}]^{2-}$ layer to ${}^{1}_{\infty}[\mathrm{ZrF_6}]^{2-}$ chains through the addition of one equivalent of fluoride.

low-dimensional transition metal halides can be interconnected through this theory (35). We recently reported the successful application of dimensional reduction to the syntheses of one-dimensional $(\mathrm{C_5H_6N})\mathrm{UO_2F_3}$ from two-dimensional $(\mathrm{C_5H_6N})\mathrm{U_2O_4F_5}$ (7, 8).

In the case of eight-coordinate uranium and zirconium fluorides, one-dimensional chains formed from edge-sharing dodecahedra are quite common, and have been observed with both inorganic and organic cations (16, 17, 36–38). The structures of $(\mathrm{C_5H_{14}N_2})_2\mathrm{U_2F_{12}}\cdot 5\mathrm{H_2O}$ (**AU1-2**) and **AU1-6** contain such chains (39). While in many cases dimensional reduction is accompanied by structural rearrangement, which complicates the prediction of new compounds from parent structures; a comparison of the structures of **AU2-6** with **AU1-6** demonstrates that these one-dimensional chains can be derived directly from the addition of one equivalent of fluoride to the two-dimensional parent structure as shown in Fig. 3. Dimensional reduction analyses of these structures may in fact provide some indication of the mechanism of formation of low-dimensional fluorides from those of higher dimensionality in hydrothermal reactions. Unfortunately, direct dimensional reduction in these systems was not observed as we did not isolate compounds containing ${}^{1}_{\infty}[\mathrm{ZrF_6}]^{2-}$ chains with ethylenediamine, or ${}^{2}_{\infty}[\mathrm{Zr_2F_{10}}]^{2-}$ sheets with piperazine.

Thermal Behavior

The thermal behavior of zirconium fluorides has been previously investigated to determine both the stability of these compounds and decomposition products (15). The thermal behavior of **AU1-6** and **AU2-6** were evaluated using differential scanning calorimetry (DSC) and thermogravimetric analysis (TGA). For our studies, we were primarily interested in differences in the dehydration temperatures that might result from the substantial differences in the structures of **AU1-6** and **AU2-6**. In fact, these thermal analyses indicate that the water molecules in **AU2-6** are more tightly bound than those in **AU1-6** as endotherms corresponding to water loss occur at 226 and 117°C in **AU2-6** and **AU1-6**, respectively.

ACKNOWLEDGMENTS

This work was supported by NASA (Alabama Space Grant Consortium) and Auburn University.

REFERENCES

1. R. J. Francis, P. S. Halasyamani, and D. O'Hare, *Chem. Mater.* **10,** 3131 (1998).
2. R. J. Francis, P. S. Halasyamani, and D. O'Hare, *Angew. Chem., Int. Ed. Engl.* **37,** 2214 (1998).
3. R. J. Francis, P. S. Halasyamani, J. S. Bee, and D. O'Hare, *J. Am. Chem. Soc.* **121,** 1609 (1999).
4. P. S. Halasyamani, S. M. Walker, and D. O'Hare, *J. Am. Chem. Soc.* **121,** 7415 (1999).
5. S. M. Walker, P. S. Halasyamani, S. Allen, and D. O'Hare, *J. Am. Chem. Soc.* **121,** 10513 (1999).
6. P. M. Almond, L. Deakin, M. J. Porter, A. Mar, and T. E. Albrecht-Schmitt, *Chem. Mater.* **12,** 3208 (2000).
7. C. E. Talley, A. C. Bean, and T. E. Albrecht-Schmitt, *Inorg. Chem.* **39,** 5174 (2000).
8. P. M. Almond, C. E. Talley, A. C. Bean, S. M. Peper, and T. E. Albrecht-Schmitt, *J. Solid State Chem.* **154,** 635 (2000).
9. P. M. Almond, L. Deakin, A. Mar, and T. E. Albrecht-Schmitt, *Inorg. Chem.* **40,** 886 (2001).
10. S. Allen, S. Barlow, P. S. Halasyamani, J. F. W. Mosselmans, D. O'Hare, S. M. Walker, and R. I. Walton, *Inorg. Chem.* **39,** 3791 (2000).
11. P. S. Halasyamani, R. J. Francis, S. M. Walker, and D. O'Hare, *Inorg. Chem.* **38,** 271 (1999).
12. R. J. Francis, M. J. Drewitt, P. S. Halasyamani, C. Ranganathachar, D. O'Hare, W. Clegg, and S. J. Teat, *Chem. Commun.* **279** (1998).
13. R. L. Davidovich, *Russ. J. Coord. Chem.* **24,** 751 (1998).
14. P. E. Ellingham, P. G. Gordon, F. Guy, and J. Rosevear, *Text. Res. J.* **53,** 577 (1983).
15. M. R. Bauer, C. R. Ross, R. M. Nielson, and S. C. Abrahams, *Inorg. Chem.* **38,** 1028 (1999).
16. C. R. Ross II, B. Paulsen, R. M. Nielson, and S. C. Abrahams, *Acta Crystallogr. Sect. B: Struct. Sci.* **54,** 417 (1998).

17. A. V. Gerasimenko, B. V. Bukvetskii, R. L. Davidovich, and N. P. Kondratyuk, *Koord. Khim.* **15,** 130 (1989).
18. R. A. Penneman, R. R. Ryan, and A. Rosenzweig, *Struct. Bonding* **13,** 1 (1973).
19. P. S. Halasyamani, M. J. Willis, P. M. Lundquist, C. L. Stern, G. K. Wong, and K. R. Poeppelmeier, *Inorg. Chem.* **35,** 1367 (1996).
20. W. T. A. Harrison, L. L. Dussack, and A. J. Jacobson, *J. Solid State Chem.* **125,** 234 (1996).
21. A. J. Norquist, K. R. Heier, C. L. Stern, and K. R. Poeppelmeier, *Inorg. Chem.* **37,** 6495 (1998).
22. M. E. Welk, A. J. Norquist, C. L. Stern, and K. R. Poeppelmeier, *Inorg. Chem.* **39,** 3946 (2000).
23. A. Rabenau, *Angew. Chem. Int. Ed. Engl.* **24,** 1026 (1985).
24. J. W. Kolis and M. B. Korzenski, *in* "Chemical Synthesis Using Supercritical Fluids" (P. G. Jessop and W. Leitner, Eds.), pp. 213–241. Wiley–VCH, New York, 1999.
25. G. M. Sheldrick, "SHELXTL PC," Version 5.0, An integrated system for solving, refining, and displaying crystal structures from diffraction data. Siemens Analytical X-Ray Instruments, Inc., Madison, WI, 1994.
26. V. Gaumet, M. El-Ghozzi, and D. Avignant, *Eur. J. Solid State Inorg. Chem.* **34,** 283 (1997).
27. D. Avignant, I. Mansouri, R. Chevalier, and J. C. Cousseins, *J. Solid State Chem.* **38,** 121 (1981).
28. A. Taoudi, A. Mikou, and J. P. Laval, *Eur. J. Solid State Inorg. Chem.* **33,** 1051 (1996).
29. J. P. Laval and A. Abaouz, *J. Solid State Chem.* **96,** 324 (1992).
30. J. R. Long, A. S. Williamson, and R. H. Holm, *Angew. Chem., Int. Ed. Engl.* **34,** 226 (1995).
31. J. R. Long, L. S. McCarty, and R. H. Holm, *J. Am. Chem. Soc.* **118,** 4603 (1996).
32. M. G. Kanatzidis and Y. Park, *Chem. Mater.* **2,** 99 (1990).
33. E. A. Axtell, J.-H. Liao, Z. Pikramenou, Y. Park, and M. G. Kanatzidis, *J. Am. Chem. Soc.* **115,** 12,191 (1993).
34. Y.-J. Lu and J. A. Ibers, *Comments Inorg. Chem.* **14,** 229 (1993).
35. E. G. Tulsky and J. R. Long, http://alchemy.cchem.berkeley.edu/.
36. J. P. Laval, D. Mercurio-Lavaud, and B. Gaudreau, *Rev. Chim. Miner.* **11,** 742 (1974).
37. J. P. Laval, R. Papiernik, and B. Frit, *Acta Crystallogr. Sect. B: Struct. Sci.* **34,** 1070 (1978).
38. R. Hoppe and B. Mehlhorn, *Z. Anorg. Allg. Chem.* **425,** 200 (1976).
39. P. M. Almond, L. Deakin, M. J. Porter, A. Mar, and T. E. Albrecht-Schmitt, *J. Solid State Chem.*, in press.